Journal of Physics: Conference Series

OPEN ACCESS

Monte Carlo simulations of the extraction of slow positrons into gas through thin SiN windows

To cite this article: B E O'Rourke *et al* 2013 *J. Phys.: Conf. Ser.* **443** 012069

Monte Carlo simulations of the extraction of slow positrons into gas through thin SiN windows

B E O'Rourke, W Zhou, N Oshima, K Ito, R Suzuki

National Institute of Advanced Industrial Science and Technology (AIST), Tsukuba, Ibaraki 305-8568, Japan

E-mail: brian-orourke@aist.go.jp, nagayasu-oshima@aist.go.jp

Abstract. Monte Carlo simulations have been performed of the extraction of slow positrons into air through thin silicon nitride (SiN) windows. The simulations are based on recent experiments at the positron probe microanalyzer (PPMA) in which slow positron microbeams have been used to analyze samples located outside the vacuum chamber in air. In the present study we calculated the fractional transmission of positrons for SiN windows as a function of positron energy and window thickness, and also calculated their energy and angular spectra after extraction. The effect of a thin air/gas layer between the window and sample was also simulated.

1. Introduction

Positrons annihilation is a unique tool for studying defects and open volumes in materials. Various experimental techniques including positron annihilation lifetime spectroscopy (PALS) have been developed and contributed to analysis and characterization over a wide range of materials [1]. Mono-energetic, low energy (slow) positrons penetrate a well defined distance into the surface layer of the sample and can be used to study thin or layered samples. Such beams of slow, monoenergetic positrons can be produced by moderation of the fast positrons produced via electron accelerators, nuclear reactors or intense radioisotope sources.

The slow positron beams are typically transported from the source to the experiment under ultra high vacuum and any samples must also be introduced into the vacuum chamber. However, for many materials it is necessary to measure outside vacuum in an environment similar to actual operational conditions. Interesting examples include wet polymer films or low-k insulating layers of electronic devices kept in humidity-controlled air or membranes in aqueous solutions. The study of powders and liquids and other samples not compatible with vacuum with low energy positrons also becomes possible.

2. The AIST Atmospheric Positron Probe Microanalyzer

A positron microbeam has been developed at AIST, Japan, the positron probe microanalyzer (PPMA). This pulsed, variable energy (1 keV – 30 keV) beam allows PALS measurements with a spatial resolution down to 30 μm and has been used for 2D and 3D defect distribution analysis [2]. The PPMA also allows the beam to be focussed on small, thin vacuum windows and hence be extracted into the air. Silicon nitride (SiN) windows were installed on the PPMA sample chamber and have been used to successfully extract slow positrons outside the vacuum chamber [3,4]. Three different windows have been used with the following dimensions; 30 nm × 0.6 mm × 0.6 mm, 200 nm × 1.5 mm × 1.5 mm and 500 nm × 3.0 mm × 3.0 mm. The density of the SiN windows is around 3.0 g/cm^3 and the compositional ratio of Si to N is approximately 1 : 1[3]. When one side of the window is evacuated to vacuum the window bends slightly towards the vacuum side. This means that a small air gap is present between the window and the sample. For the 30 nm and 200 nm windows this minimum air gap, d_0, was measured using a laser microscope to be 35 μm – 40 μm and 65 μm – 70 μm respectively. The deflection of a clamped film when $d_0 >> h$, can be approximated by the expression $d_0 \approx \left(r^4 P / Eh\right)^{1/3}$ [5], where r is the radius, P the applied pressure (1 atm), E the Young's modulus and h the material thickness. For CVD prepared SiN films a value of E = 270 GPa has been reported [6]. Assuming a value for the radius, r, equal to half the lateral dimension, values of d_0 = 37, 85 and 312 μm for the 30, 200 and 500 nm films respectively are calculated, in reasonable agreement with the measured value for the thinner two films.

When the slow positron beam passes through the SiN window it will interact and some fraction of the incident positrons will be backscattered, some annihilated in the window and some fraction transmitted. The transmitted beam will emerge with an energy distribution and angular dispersion. Although stopping profiles in multilayer systems can be estimated by scaling laws [7], Monte Carlo simulations can be used to determine energy and angular distributions alongside stopping profiles. The present report aims to estimate these effects at the AIST atmospheric PPMA using the Penelope2008 code [8]. Penelope 2008 provides full support for positron interactions and can simulate processes with energies down to several hundred eV.

3. Monte Carlo Simulations

3.1. Slow positron transmission through SiN

In the initial simulation a slow, monoenergetic positron beam at normal incidence to a thin SiN film was simulated and the positron transmission fraction and energy and angular distributions of transmitted positrons calculated.

3.1.1 Positron Transmission Fraction

A typical simulation result is shown in figure 1 where the relative fractions of transmitted, backscattered and absorbed (annihilated) positrons are plotted as a function of positron energy for the 200 nm thick SiN window. The transmitted fraction increases from 0 around 3 keV to almost 100% at 30 keV. The backscattered fraction decreases from around 10% at 5 keV to less than 1 % at 30 keV.

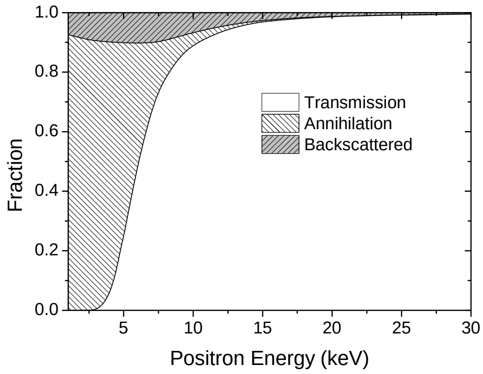

Figure 1. Fractional transmission, back-scattering and ab-sorption (annihilation) of positrons incident on a 200 nm SiN film as a function of positron energy.

Although other profiles have also been shown to give good agreement with measurements [9] the stopping profile, P, of positrons in materials is typically characterised by the Makhov profile [10];

$$P(z,E) = -\frac{\mathrm{d}}{\mathrm{d}z}\exp\left[-\left(\frac{z}{z_0}\right)^m\right] \text{ with } z_0 = \frac{AE^n}{\rho\,\Gamma(1+1/m)} \tag{1}$$

A, *n* and *m* are material and energy dependant parameters [11], *E* is the energy in keV and *z* the material thickness in nm. ρ is the material density (in g/cm^3) and Γ is the Gamma function. Neglecting backscatter, the transmission through a film of a certain depth can be estimated by integrating this function. We can then fit our simulation results to this integral to find the parameters for SiN.
Using the transmission fractions calculated via the Monte Carlo simulation gives the following result for these parameters (with $m = 2$); $A = 32.8 \pm 0.6$, $n = 1.66 \pm 0.01$. Figure 2 shows the simulation results for positron transmission through various thicknesses of SiN films plotted alongside curves generated with the calculated fit parameters.

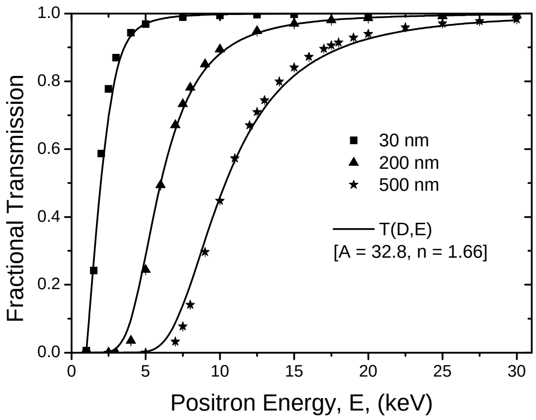

Figure 2. Plot of the calculated transmission of positrons through thin SiN films as a function of positron energy and film thickness and compared to curves generated by an integral of the Makhov profile with the parameters *A* = 32.8, *n* = 1.66, *m* = 2.

3.1.2 Energy and angular distribution of transmitted positrons

The initially monoenergetic and parallel positron beam will emerge with broad energy and angular distributions. Figure 3a shows the calculated energy profile of initially 5 keV positrons transmitted through both 30 nm and 200 nm SiN films. At 5 keV the transmission through 30 nm films is 97% while that for 200 nm films is 24%. For the thicker 200 nm film it is seen that a broad energy distribution which peaks around 3.5 keV is obtained whereas for the thinner 30 nm film the distribution is more sharply peaked with a maximum at 4.9 keV. An estimate for the width of the distribution (E_-, E_+) can be obtained by finding the energy at which the probability is half of this maximum value (N[$E_\pm$] = 0.5 N[E_{peak}]). This analysis was repeated for a range of impact energies at the three SiN film thicknesses, 30 nm, 200 nm and 500 nm and is plotted in figure 3b. The error bars in this figure represent the distribution width. As the positron energy is increased the energy distribution width narrows and approaches the initial impact energy.

The angular distribution of transmitted/backscattered positrons is shown in figure 4. The number of positrons emitted at a function of polar angle, θ, is given by the probability per steridian (ε) multiplied by the factor 2πsin(θ). In figure 4a this quantity is plotted for a positron beam of 5 keV energy incident on 30 nm and 200 nm SiN films. In both cases the distribution peaks at a particular angle (θ_{max}) and then decays with increasing angle to zero at 90° (perpendicular to the film). The distribution between 90° and 180° corresponds to positrons backscattered from the film. The angle where 2πsin(θ)ε reaches a maximum, θ_{max}, is plotted as a function of positron energy for the 30 nm, 200 nm and 500 nm SiN films in figure 4b. This angle decreases with decreasing window thickness and increasing positron energy. For the 30 nm window, θ_{max} is less than 5° for E > 10 keV.

3.1.3. Temporal and Spatial Resolution at the sample

Using the results from the previous section it is possible to estimate the effect of the SiN window on the temporal resolution. A simple estimate is to calculate the time difference of arrival at the sample between the high energy and low energy positrons. For this analysis we define the high energy and low energy values as the energy at which the probability is half of peak value (N[$E_{\pm}$] = 0.5 N[E_{peak}]). We also define the distance positrons travel between the SiN window and sample as equal to the minimum gap d_0 divided by the cosine of the peak angle θ_{max}. The pulse broadening, ΔT, is then given by,

$$\Delta T = \frac{d_0}{\cos\theta_{\max}}\left(\frac{1}{\sqrt{2E_-/m}} - \frac{1}{\sqrt{2E_+/m}}\right), \tag{2}$$

and the results plotted in figure 5a.
It is clear that even for very low energy positron beams (≥ 1keV) the reduction in temporal resolution is only a few ps and is therefore expected to have no significant influence on the final temporal resolution.

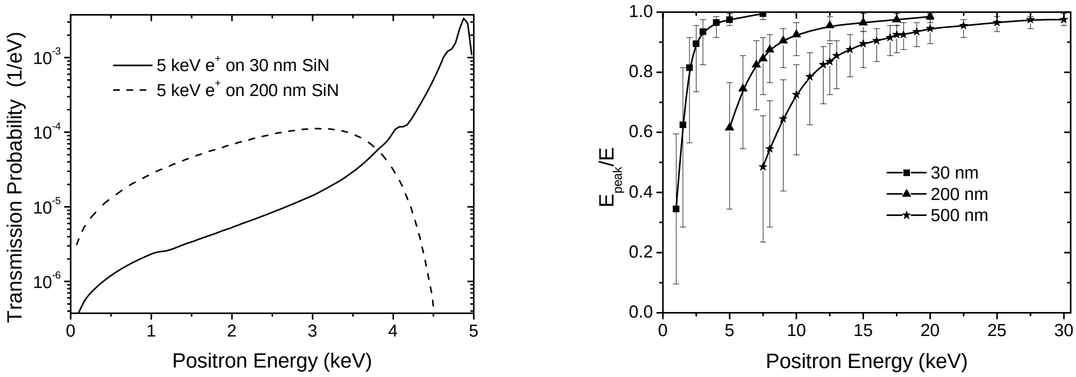

a) b)

Figure 3. a) Energy distribution of initially 5 keV positrons transmitted through 30 nm and 200 nm SiN films. **b)** E_{peak} of transmitted positrons and distribution width (N[$E_{\pm}$] = 0.5 N[E_{peak}]) shown by the error bars plotted as a function of incident positron energy for transmission through 30 nm, 200 nm and 500 nm SiN films.

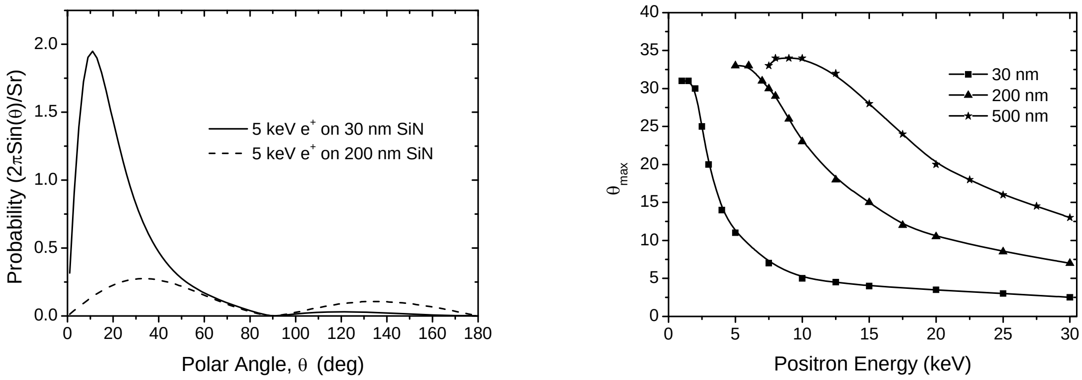

a) b)

Figure 4. a) Angular distribution of initially 5 keV positrons transmitted/backscattered through 30 nm and 200 nm SiN films. **b)** The angle of peak positron emission, θ_{max}, plotted as a function of incident positron energy for transmission through 30 nm, 200 nm and 500 nm SiN films.

We can also estimate the positron beam size on the sample. If we assume the initial beam diameter, w_0, as 30 μm, the spot size on target can be estimated by; $w = w_0 + 2d_0 \tan\theta_{\max}$. The result of this calculation is shown in figure 5b. The reduction in beam size resolution is estimated to be quite small, especially when the thinnest (30 nm) window is used over a wide energy range.

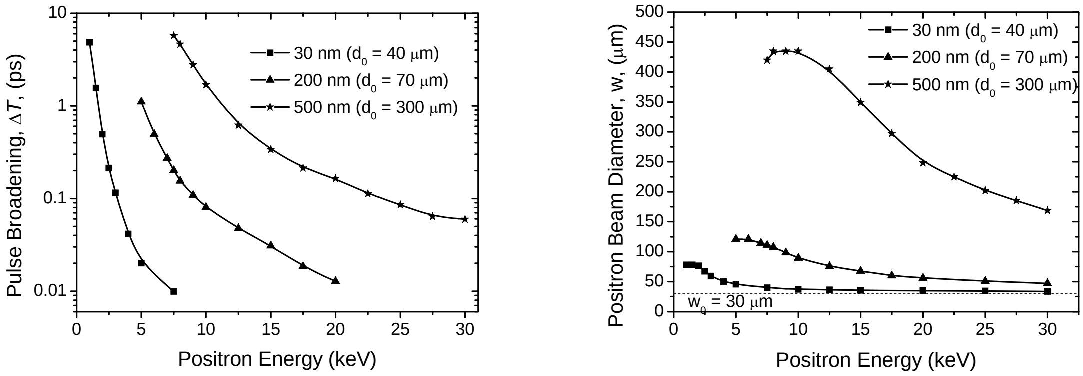

a) b)

Figure 5. a) Estimate of the pulse broadening, ΔT, caused by positrons passing through the SiN window. ΔT is estimated using the minimum window-sample gap, d_0, the width of the energy distribution and the angle of maximum positron emission, θ_{max}. b) Estimated size of the positron beam spot on target based on θ_{max} and the minimum window – sample gap, d_0. For the 30nm and 200nm windows d_0 is based on the value measured using a laser microscope whereas for the 500 nm window a value of 300 μm was assumed based on the calculation in section 2.

3.2. Effect of air/gas layer

As mentioned in section 2, due to the curvature of the SiN window when one side is under high vacuum, a thin layer of air (or gas) will be present between the SiN window and the sample. This layer will also cause a loss of transmission and broadening of the energy and angular distributions.

If we consider the SiN – Gas layer – Sample as a multilayer system, the stopping probability η_i of positrons in the i-th layer is given by [1,3];

$$\eta_i = \int_{x_i}^{x_{i+1}} P_i(z,E)\,\mathrm{d}z \ , \quad P_i(z,E) = -\frac{\mathrm{d}}{\mathrm{d}z}\exp\left[-\left(\frac{z-\delta z_i}{z_{0i}}\right)^m\right] \text{ with } z_{0i}\Gamma\left(1+\frac{1}{m}\right) = \frac{A_i E^{n_i}}{\rho_i}\ , \tag{3}$$

where P_i is the stopping profile of positrons in the i-th layer and z(nm) is the depth from the surface of the top layer. The depth correction factor δz_i is given by [3];

$$\delta z_i = \begin{cases} x_i - z_{0i}\left[-\ln\left(1-\sum_{k=1}^{i-1}\eta_k\right)\right]^{\frac{1}{m}} & \text{for } i \geq 2 \ , \\ 0 & \text{for } i = 1 \end{cases} \tag{4}$$

where x_i is the depth from the surface to the interface between the $(i-1)$-th and the i-th layers.

Figure 6 shows the result of simulations based on a recent experiment involving a polyvinyl alcohol (PVA) film. In this experiment the 30 nm SiN window was used together with a 35 μm Kapton spacer to give a window – sample separation of 70 μm. N_2 gas at 1 atm was present in this region. Monte Carlo calculations based on this geometry were performed and the fraction stopped in each layer (after removal of the small fraction backscattered from the SiN window) was determined. Also shown in the figure is the calculated stopping probability (or absorbed fraction) in each layer based on the model outlined above. This model tends to slightly overestimate the absorption in the PVA sample and underestimate the absorption in the N_2 layer but overall agreement is good indicating that this model can be used as a guideline for future experiments.

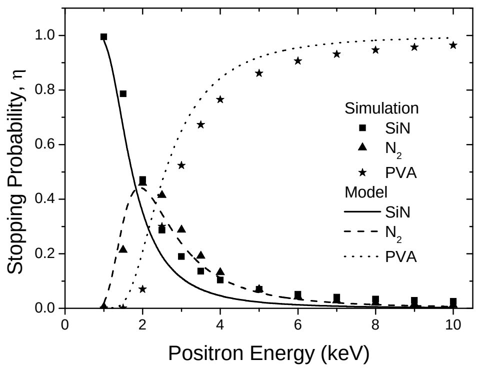

Figure 6. Plot of the calculated stopping probability in each layer [SiN (30 nm), N_2 (70 μm), PVA (2 mm)] as a function of positron energy. Also shown is the stopping probability based on the multi-layer Makhov model with typical values of the free parameters (A = 40, n = 1.6) for each layer [10].

4. Summary

Monte Carlo simulations of the transport of low energy positron beams through thin SiN windows and gas layers have been performed. The simulations were motivated by the recent development of an atmospheric positron probe microanalyzer at our institute whereby a focussed positron beam is extracted from the vacuum into air. It was found that the transmission of slow, monoenergetic positrons through SiN can be modelled using the well known Mahkov profile. The simulations also suggested that the effect of extraction through SiN windows on the temporal resolution in PALS is insignificant. For the lateral beam size on target some degradation is expected but a lateral resolution less than 100 μm should be possible using the thinner (30 μm) SiN windows over a wide energy range.

Acknowledgement: This work was supported by NEDO. The SiN shape measurement was supported by the AIST Nano-Processing Facility.

5. References

[1] Coleman P 2000 *Positron Beams and Their Applications* (Singapore: World Scientific)
[2] Oshima N, Suzuki R, Ohdaira T, Kinomura A, Narumi T, Uedono A and Fujinami M 2008 *J. Appl. Phys.* **103** 094916; 2009 *Mat. Sci. Forum* **607** 238; 2009 *Appl. Phys. Lett*. **94** 194104
[3] Oshima N, O'Rourke B E, Kuroda R, Suzuki R, Watanabe H, Kubota S, Tenjinbayashi K, Uedono A and Hayashizaki N 2011 *Appl. Phys. Express* **4** 066701
[4] Zhou W, Chen Z, Oshima N, Ito K, O'Rourke B E, Kuroda R, Suzuki R, Yanagishita H, Tsutsui T, Uedono A and Hayashizaki N 2012 *Appl. Phys. Lett.* **101** 014102
[5] Landau L D and Lifshitz E M 1986 *Theory of Elasticity 3rd Edition* (Oxford: Butterworth) pp 53
[6] Pierson H O 1999 *Handbook of Chemical Vapor Deposition (CVD): Principles, Technology, and Applications 2nd Edition* (William Andrew Publishing)
[7] Aers, G C 1994 *Appl. Phys. Lett.* **64** 661
[8] Baro J, Sempau J, Fernandez-Varea J and Salvat F 1995 *Nucl. Instrum. Methods Phys. Res. B* **100** 31; see http://www.nea.fr/tools/abstract/detail/nea-1525
[9] Baker J A, Chilton N B, Jensen K O, Walker A B, Coleman P G 1991 *J. Phys.: Condens. Matter* **3** 4109
[10] Mills A P Jr and Wilson R J 1982 *Phys. Rev. A* **26** 490; Valkealahti S and Nieminen R M 1983 *Appl. Phys. A* **32** 95-106; Vehanen A, Saarinen K, Hautojärvi P and Huomo H 1987 *Phys. Rev. B* **35** 4606-4610
[11] Algers J, Sperr P, Egger W, Kogel G and Mauer F H 2003 *Phys. Rev. B* **67** 125404